Trend Modeling Techniques and Guidelines

Jason A. M^{c}Lennan, Oy Leuangthong,
and Clayton V. Deutsch

Centre for Computational Geostatistics (CCG)
Department of Civil and Environmental Engineering
University of Alberta

Abstract

A petroleum reservoir or mining deposit is an economic concentration of hydrocarbon or mineral resulting from a unique sequence of depositional events. This geological history is manifested through spatial trends in existing reservoir or deposit properties. Stratigraphic surface elevations, layer thickness, petrophysical properties, and mineral grades can all display trends in a single setting. These smooth variations must be reproduced in any legitimate model of heterogeneity. Conventional geostatistics will reproduce the sample data, its distribution, and the model of spatial correlation; however, there are often too few data to satisfactorily reproduce the trend. Geostatistical workflows must then be modified to explicitly account for the trend.

The overall workflow for uncertainty characterization with a significant trend involves two major steps: (1) modeling the trend and (2) incorporating the trend into geostatistical operations. Numerous techniques and algorithms are available to construct trend models. There are also several options to consider for integrating trend models into geostatistical workflows. Industry and practitioners are becoming overwhelmed with the alternatives. There is a need to synthesize these methods and provide guidelines for implementation. This paper addresses this need. The procedures and implementation details for constructing trend models and integrating trends into geostatistical workflows are presented with various petroleum and mining examples.

1. Introduction

The spatial distribution of a geological variable is of dual character: partly structured and partly stochastic. The structured component is necessitated by a unique set of interpretable depositional events that originally concentrated the hydrocarbon or mineral; the stochastic component is due to random fluctuations in these geological formation processes. Actually, Georges Matheron invented the name and field of geostatistics on the basis of this observation:

> … even though mineralization is never so chaotic as to preclude all forms of forecasting, it is never regular enough to allow the use of a deterministic forecasting technique. This is why (at least, simply realistic) estimation must necessarily take into account both features – structure and randomness – inherent in any deposit. Since geologists stress the first of these two aspects, and statisticians stress the second, I proposed, over 15 years ago, the name geostatistics… (Journel, 1978).

This notion of dual character can be represented analytically. Consider the random function $Z(\mathbf{u})$ consisting of the set of random variables $Z(\mathbf{u}_\alpha)$ defined at each time and location $\mathbf{u}_\alpha$ within some

time and space domain A: $Z(\mathbf{u}) = \{Z(\mathbf{u}_\alpha), \forall \mathbf{u}_\alpha \in A\}$. If the random variable $Z(\mathbf{u}_\alpha)$ represents a geological variable, each one can be decomposed into a structured and random component:

$$Z(\mathbf{u}_\alpha) = m(\mathbf{u}_\alpha) + r(\mathbf{u}_\alpha) \quad (1)$$

where m is the structured component and r is the random component. The structured component m is referred to as the trend and the random component r is referred to as the residual. This analytical decomposition of a geological variable is intriguing in that (1) it is a simple mathematical signature of the birth of geostatistics, (2) it explains the spatial character of virtually any geological random variable encountered in petroleum and mining applications, and (3) it is at the heart of any modern approach for integrating trend models into geostatistical workflows.

Formula (1) is indeed the basis for much of the work in this paper. We emphasize and explore the available methods for deriving the trend component $m(\mathbf{u}_\alpha)$. Implementation details, examples, and recommendations will enforce the understanding of the available techniques. Once the trend $m(\mathbf{u}_\alpha)$ is modeled, it is integrated into geostatistical operations. We also explore the available methods and options available for incorporating trend models into practical geostatistical workflows through descriptions and various examples.

2. Trend Definition

Virtually any geological attribute $Z(\mathbf{u}_\alpha)$ has a structured or trend component $m(\mathbf{u}_\alpha)$ of spatial variability since its concentration was guided within the existing reservoir or deposit according to a unique sequence of depositional events and structural deformations that are governed by the physical and geological laws of nature. From those laws, practitioners are able to rationalize and understand trends. For example, consider the two layer reservoir with a marine layer overlying an estuary layer in Figure 1. We expect higher porosities at the bottom of the reservoir since we understand that relative to the marine environment, the estuarine environment would have had higher saline content and correspondingly higher porosities.

A trend $m(\mathbf{u}_\alpha)$ is defined as a gradually varying expectation of the variable $Z(\mathbf{u}_\alpha)$ over the time and/or space interval, A, discretized by $\mathbf{u}_\alpha$. The following series of examples illustrates this definition. Let $Z(\mathbf{u}_\alpha)$ be the distribution of crude oil price ($US/barrel) on the NYMEX in the year 2004 shown in Figure 2. Notice the gradual increase in crude oil price from approximately $35US/barrel in January to approximately $50US/barrel in December. This allows $Z(\mathbf{u}_\alpha)$ to be interpreted as the sum of a trend $m(\mathbf{u}_\alpha)$ and residual $r(\mathbf{u}_\alpha)$ component at all times $\mathbf{u}_\alpha$ within the year 2004. Now let $Z(\mathbf{u}_\alpha)$ be the log derived porosity profile in the elevation interval shown in Figure 3. Similarly, $Z(\mathbf{u}_\alpha)$ can be interpreted as the sum of a trend $m(\mathbf{u}_\alpha)$ and residual $r(\mathbf{u}_\alpha)$ component for all elevations $\mathbf{u}_\alpha$ within the logging interval. Finally, consider some type of revenue variable derived partly from both the crude oil prices in Figure 2 and the porosities in Figure 3. Here, we can interpret a time and space dependent trend toward higher revenues for times later in the 2004 year and locations lower in elevation. Practically therefore, a trend can be observed in 4 Dimensions (1D time + 3D space). In this work, only the 3D space domain is considered.

3. Modeling Principles

Interpreting a trend is highly dependent on the scale or domain A. In Figure 2, the domain A consists of all the times $\mathbf{u}_\alpha$ in the year 2004; however, if we instead take A to be the month of June, we would actually interpret a decreasing crude oil price trend. In Figure 3, if A were to consist of just the elevations $\mathbf{u}_\alpha$, in between the two horizontal red lines, we would interpret no trend at all. The interpretation clearly depends on the scale of consideration, that is, the limit values of $\mathbf{u}_\alpha$ in A.

The form of the trend $m(\mathbf{u}_\alpha)$ must be reproduced at all locations $\mathbf{u}_\alpha$ in A in any realistic model of heterogeneity; however, data paucity makes this a significant challenge. Although it may be straightforward to interpret a trend from the data and geological principles, it may be difficult to satisfactorily reproduce this trend in estimation or simulation using the sample data alone. Figure 4 shows a vertical string of grid blocks to be estimated from two log porosity profiles each a distance **h** away. From the porosity profiles and knowledge of a geological setting similar to that described in Figure 1, the trend $m(\mathbf{u}_\alpha)$ component can be inferred for the unestimated grid blocks. The form of this trend should be reproduced in estimation; however, there is no guarantee of this using just the two porosity profiles. In particular, if **h** is beyond the range of spatial correlation, the trend could be misrepresented. To enforce the correct form of $m(\mathbf{u}_\alpha)$, therefore, the practitioner is forced to explicitly model the trend at all locations $\mathbf{u}_\alpha$ within the domain A.

The amount of variability modeled by the trend $m(\mathbf{u}_\alpha)$ is a subjective balance between deterministic knowledge and stochastic fluctuation. Of course, our deterministic understanding of the geology governing the formation of a reservoir or deposit is subjective. In all cases, the trend should model no more variability than what our deterministic understanding of the geological processes suggests; nevertheless, in practice, the trend is often over-fit and represents too much variability. Consider again the estimation scheme in Figure 4. Recall the trend $m(\mathbf{u}_\alpha)$ component based on our understanding of the depositional setting. There is an understandable geological rationale (see Figure 1) to expect an increasing porosity profile at the unestimated grid blocks. However, it is easy to let the neighboring porosity profiles over-influence a trend model without any additional deterministic knowledge. Incorporating too much variability in the trend dangerously leaves too little variability to the random fluctuations inherent in all earth sciences variables that are modeled by stochastic methods such as geostatistics.

The subjective nature of trends has led to a surplus of available techniques for building a locally varying mean model $m(\mathbf{u}_\alpha)$. A continuum of trend modeling techniques is available. Each method has its own advantages and disadvantages, implementation details, and range of applicability. The implementation of each method varies according to the application. And certainly there are some techniques better suited to certain petroleum reservoir or mining deposit scenarios. There is a need for this information to be well documented and transparent to practitioners.

4. Techniques and Guidelines

A variety of trend modeling techniques ranging from the most conventional to the most modern are investigated in this work. With respect to this range, we investigate (1) hand mapping, (2) moving window averages, (3) inverse distance schemes, (4) simple kriging, (5) block kriging, (6) universal kriging, and (7) probability combination schemes in particular. All of the methods strive to model the smoothly varying expectation of the attribute of interest $m(\mathbf{u}_\alpha)$. For each technique, a description, example, and some implementation guidelines are illustrated.

4.1. Hand Mapping

The most conventional approach to trend modeling is human interpretation or hand mapping and contouring. This process usually involves the digitization of hand-drawn contour lines. The contour lines are digitized on screen and the lines are converted to points. These points can be considered alone to explicitly produce the trend model or appended to the existing data to implicitly account for the trend in estimation.

Although hand mapping techniques are flexible in allowing the pratictioner to model virtually any hint of smoothly varying spatial structure, there are a number of disadvantages. Most importantly, these methods are not repeatable and difficult to adjust when faced with new data or information. A significant amount of professional time and effort are also required to avoid creating artifacts, that is, ensuring a horizontal trend makes physical sense with respect to a vertical trend.

Modern computing power has quickly made hand mapping techniques obsolete. Moreover, reservoirs or mines that use hand mapping techniques are more likely to simply use these maps for resource characterization than use them within a more complex trend modeling approach. There are few current examples of good hand mapping implementations. In virtually all situations, an automated method is preferred due to efficiency and repeatablility.

4.2. Computer Mapping

Contouring has become largely automated and increasingly sophisticated with the advancement of computing power and geostatistical research and development. Several methods are available to create smoothly varying maps of virtually any variable. The methods investigated in this paper are, in order of increasing complexity, moving window averages, inverse distance estimation, simple kriging, block ordinary kriging, and universal kriging for the mean. All of the methods are conditioned to all available sample data.

Moving Window Averages

The first method discussed is a moving average method. These methods average the attribute of interest within 1D intervals, 2D windows or 3D cubes that translate over the span of the reservoir or deposit. The attribute of interest can be a continuous or categorical variable. A geometric or power law average can be used for permeability.

Figure 6 shows a categorical variable example in a petroleum reservoir scenario. There are 9 facies types including sand. The proportion of sand is calculated within 15m vertical windows from the bottom to the top of the reservoir. The proportion is then plotted against the center of each elevation bin in Figure 6. The results suggest there is a significant tendency for higher sand proportions in the middle of the reservoir.

Moving window averages are simple and effective trend modeling techniques. They can be applied at any dimension. The corresponding intervals, windows, or cubes can be made large and/or can overlap when there are too few data to obtain smoothly varying results. Moving window averages, however, do not apply any type of weighting scheme to the sample data, that is, all of the samples within the averaging limits receive the same weight. Therefore, these techniques may not be inappropriate in situations when data are clustered along well or drillhole strings.

Inverse Distance

Inverse distance is a grid estimation procedure that weights surrounding data inversely based on their distance from the estimation location. The grid can be in one, two, or three dimensions.

Samples that are further away from the estimation location receive less weight; the severity of the weighting is controlled by raising the inverse distance to a user-defined power. A search routine determines the number of data to retain. It is possible to incorporate simple anisotropy.

Figure 7 shows a 2D aerial example using gold grade from a synthetically created mining database. The inverse distance method is applied to the vertical gold grade averages within each drillhole. The inverse distances are raised to a moderate power of 1.0 and the closest 50 data are retained to estimate each grid block. The results suggest there is a tendency for higher gold grade in the southern edge of the area. The sample data can be easily seen where they are reproduced at their locations.

Inverse distance weighting is also a simple and effective trend modeling technique. A large search routine retaining many data and the calibration power give inverse distance schemes the flexibility to create smoothly varying maps in many practical situations. However, these methods do not explicitly account for the model of spatial correlation from variography and do not account for the redundancy between sample data. Inverse distance techniques then may not be appropriate when complex anisotropy or significant clustering exists.

Simple Kriging

Simple kriging is a weighted linear estimation technique that calculates the weighting scheme for surrounding data to minimize the expected error variance at each estimation location. This method simultaneously accounts for closeness of sample data to the estimation location and the redundancy of data in terms of the spatial correlation modeled by the variogram. The search for data is also done in terms of correlated distance.

For the same vertically averaged conditioning data used for the inverse distance scheme, a simple kriging implementation is shown in Figure 8. The data locations are less obvious. An anisotropic variogram with a major northeast direction of continuity is used. The same number of data (50) is retained as in the inverse distance weighting scheme; however, different data are retained due to the anisotropic search routine. The same tendency for high gold grade in the southern portion of the area is apparent; however, the continuity of these high values is aligned in the northeast direction.

Simple kriging is a very effective trend modeling technique. The method can be applied to any attribute of interest for virtually any petroleum or mining scenario. However, the results are sensitive to the assumption of stationarity, that is, only one mean value can be applied within the entire estimation area.

Block Ordinary Kriging

Ordinary kriging is an increasingly popular trend modeling technique. Ordinary kriging is a variation of simple kriging where the sum of the weights assigned to the data must equal 1.0. Essentially this requires the mean to be re-calculated at each estimation location separately. This is preferred for many practitioners since it relaxes the stationarity assumption. A block discretization and significant nugget effect are used to ensure the block estimates are smoothly varying.

Figure 9 shows an example of ordinary kriging for building a 3D trend model. The sections shown are central plan view slices. A synthetic 3D sample dataset was created to condition 6 different block ordinary kriging runs. Each run corresponds to a different nugget effect and range for an isotropic variogram. A 4 x 4 x 4 block discretization is used for each run. Although the

resulting maps do not seem to be very sensitive to the variogram parameters, the 45% nugget effect and 48 range case produces the smoothest variation.

Ordinary kriging is a very effective and robust trend modeling technique. A large search routine retaining many data, a high block discretization, and high variogram nugget and range can effectively model any smooth variation in any attribute of interest for virtually any petroleum or mining scenario.

Universal Kriging

Universal kriging incorporates a functional form of the trend for each direction into kriging estimates. Usually, the functional form of the mean is input and the residuals at the data locations are estimated and added back to the mean. However, to use universal kriging for trend modeling, the mean model or trend can be estimated. The only additional requirement to implement universal kriging is the parameterization of the functional form of the mean.

Figure 10 shows a simple example to illustrate the process. There are 3 data trending towards high grades in the *X* direction. Three different functional forms of the mean in the *X* direction are considered: (1) constant (top row), (2) linear (middle row), and quadratic (bottom row). The second and third column shows the estimated mean as well as the estimated attribute of interest using the locally varying mean model, respectively. It is important to use the entire dataset when using universal kriging; otherwise, artifacts may be created in the trend model. Figure 11 shows a universal kriging implementation using the same data as the ordinary kriging example. Here a 25% nugget and 36 range isotropic variogram are used. A linear drift in the *XY* direction is parameterized. The corresponding trend does not result in such extreme trend values as that shown in Figure 9.

It is not recommended to use universal kriging to estimate the trend model. The procedure is not as straightforward as the previous methods described and takes much longer since the global database needs to be retained to estimate the mean model at each grid block location. Moreover, these disadvantages are not associated with measurable improvement.

4.3. Combining Lower Order Trends

The general approach to trend modeling is to build one, two, or three lower dimensional trend models and then combine them into the desired 3D locally varying mean model. Any one of the previously discussed methods could be used to model a 2D or 1D trend model. There are some different methods available to combine lower order trends into a full 3D trend. These methods are referred to as probability combination schemes. Some different probability combination schemes are investigated and discussed in this section.

Consider inferring the probability of some event A through its conditional probability P(A | B, C) to two separate events B and C. The A, B and C events are unconstrained as long as the conditional probabilities P(A), P(A | B) and P(A | C) can be evaluated. The challenge is how to combine the prior P(A) and pre-posterior P(A | B) and P(A | C) conditional probabilities to infer the posterior P(A | B, C) probability. There are two common combination approaches: (1) full independence, which assumes B and C are fully independent and (2) permanence of ratios, which assumes B and C are incrementally conditionally independent. Appendix A develops and explains the analytical formulation of these two probability combination schemes. Formula (2) and (3) show the results for full independence and permanence of ratios, respectively.

$$P(A \mid B,C) = \frac{P(A) \cdot P(B \mid A) \cdot P(C \mid A)}{P(B,C)} \tag{2}$$

$$P(A \mid B,C) = \frac{P(A) \cdot P(B \mid A) \cdot P(C \mid A)}{P(A) \cdot P(B \mid A) \cdot P(C \mid A) + P(\tilde{A}) \cdot P(B \mid \tilde{A}) \cdot P(C \mid \tilde{A})} \tag{3}$$

$$= \frac{\dfrac{P(A \mid B) \cdot P(A \mid C)}{P(A)}}{\dfrac{P(A \mid B) \cdot P(A \mid C)}{P(A)} + \dfrac{P(\tilde{A} \mid B) \cdot P(\tilde{A} \mid C)}{P(\tilde{A})}}$$

where Ã is the complement of event A. Consider the following event and probability definitions (also illustrated in Figure 12):

- Event B is the probability of sand facies at a particular 2D horizontal grid cell location:

$$P(A \mid B) = p_{S(x,y)}$$

- Event C is the probability of sand facies at a particular 1D vertical grid cell location:

$$P(A \mid C) = p_{S(z)}$$

- Event A is the probability of sand facies at a particular 3D grid cell location:

$$P(A) = p_S \quad ; \quad P(A \mid B,C) = p_{S(x,y,z)}$$

where p_S represents probability of sand and the x, y, z indices define the grid cell locations. The probability of an indicator variable is its mean; therefore, spatial p_S probabilities are interpreted as locally varying means or trend models. Figure 12 also shows a pre-posterior $p_{S(x,y)}$ horizontal trend map and a pre-posterior $p_{S(z)}$ vertical trend curve. The challenge is then to combine the lower dimensional $p_{S(x,y)}$ and $p_{S(z)}$ pre-posterior probabilities (and prior probability p_S) into a 3D posterior $p_{S(x,y,z)}$ trend model suitable for simulation.

The first example is the combination of a 2D horizontal and a 1D vertical sand facies trend into a 3D trend model. The pre-posterior P(A | B) and P(A | C) probabilities are shown in Figure 13. P(A | B) was created using simple kriging and P(A | C) was created using a moving window average. Full independence and permanence of ratios is used for combination. Figures 14 and 15 show the resulting full independence and permanence of ratios posterior probability models for a high probability case (Z=30m) and low probability case (Z=90m). Note that both seem to exaggerate the highs and lows, but the permanence of ratios hypothesis is not as severe.

The full independence and permanence of ratios combination schemes in Equations (2) and (3) are for combining probabilities. It was straightforward to develop them within a facies trend modeling framework since the mean of an indicator is in fact a probability; however, relations (2) and (3) do not hold for units of continuous variables such as mineral grades or permeability. The challenge then is to extend the full independence and permanence of ratio combination schemes in (2) and (3) to include continuous variables.

We propose using the cumulative distribution function (cdf) of the continuous variable to get the prior and pre-posterior probabilities for combining into a posterior probability. The method is illustrated in Figure 16. Consider the following probability and event definitions for a continuous variable w:

- Event B is the cdf value of w at a particular 2D horizontal grid cell location:

$$P(A \mid B) = F(w_{(x,y)})$$

- Event C is the cdf value of w at a particular 1D vertical grid cell location:

$$P(A \mid C) = F(w_{(z)})$$

- Event A is the cdf value of w at a particular 3D grid cell location:

$$P(A) = \overline{w} \quad ; \quad P(A \mid B, C) = F(w_{(x,y,z)})$$

where F represents the cdf of the continuous w variable and the x, y, z indices define the grid cell locations. The cdf function F(w) is used to get the input prior and pre-posterior probabilities from original w units for combining into the posterior probability. The inverse cdf function $F^{-1}(w)$ is then used to get back the original w units of the posterior probability. By using cdf values, the full independence and permanence of ratios hypotheses can be used for trend modeling on continuous variables.

5. Geostatistics with a Trend

Once a locally varying mean or trend model is constructed using an appropriate technique, several options are then available for integrating the trend into a geostatistical workflow. Although this work does not emphasize this phase of handling trends, these options are briefly discussed along with some implementation details and guidelines.

5.1. Stationarity

Geostatistics is increasingly popular for mapping regionalized variables in the petroleum and mining industry. These tools provide the ability to construct multiple equally probable and geologically realistic models of heterogeneity that can honor several types of conditioning information. These models can be used to assess the uncertainty of various production performance variables. Conventional geostatistics (or any statistical inference), however, is limited by stationarity which is manifested from a limited set of sample data.

The incorporation of trend modeling into geostatistical frameworks is challenging due to stationarity. Stationarity is not a characteristic or property of a reservoir or deposit nor is it a testable hypothesis. It is a decision made by the practitioner that amounts to assuming the geological phenomenon is homogeneous within some intermediate domain A′ within the full domain A. Consider a vector of N sample data from A, $z(\mathbf{u}) = \{z(\mathbf{u}_\beta), \forall \mathbf{u}_\beta \in A, \beta = 1,..., N\}$. Strict stationarity assumes invariance of the multivariate cumulative distribution function (cdf) under any translation **h** over the domain A:

$$F_{Z(\mathbf{u}_1),\ldots,Z(\mathbf{u}_N)}\left(z(\mathbf{u}_1),\ldots,z(\mathbf{u}_N)\right) = F_{Z(\mathbf{u}_1+\mathbf{h}),\ldots,Z(\mathbf{u}_N+\mathbf{h})}\left(z(\mathbf{u}_1+\mathbf{h}),\ldots,z(\mathbf{u}_N+\mathbf{h})\right) \qquad \forall \mathbf{h} \qquad (2)$$

However, since only first and second order moments are needed in conventional (linear) geostatistics, only second order stationarity is required. In particular, this entails:

1. The mean is independent of location,

$$E\left\{Z(\mathbf{u}_\alpha)\right\} = m \qquad \forall \mathbf{u}_\alpha \in A' \qquad (3)$$

2. The covariance is independent of location and depends only on the lag vector **h**,

$$C\left(Z(\mathbf{u}_\alpha), Z(\mathbf{u}_\alpha+\mathbf{h})\right) = C(\mathbf{h}) = E\left\{Z(\mathbf{u})\cdot Z(\mathbf{u}+\mathbf{h})\right\} - m^2 \qquad \forall \mathbf{u}_\alpha \in A' \qquad (4)$$

The decision of stationarity is required for geostatistical inference. In this way, it is referred to as an export license. For instance, if we assume Z(**u**) is a Gaussian random function, we can fully define each Z($\mathbf{u}_\alpha$) with its mean and variance from the z(**u**) data vector by assuming only second order stationarity.

Trends are non-stationarities and directly violate any decision of stationarity. Perhaps it is ironic that the creation of geostatistics based on Equation (1) suggests a trend component whereas the implementation of modern geostatistics in Equation (3) requires there to be no trend. Therefore, although geostatistical estimation and simulation methods are able to honor various types of conditioning information, some modifications to the classical workflows are required to adequately reproduce a trend.

Just as there are several options to consider for building a trend model, there are also several options to consider for incorporating this trend model into a geostatistical framework. The options available and some associated implementation details and guidelines are now considered. The methods can be summarized into two categories: (1) a classic decomposition, and (2) a stepwise transformation.

5.2. Classic Decomposition

The most common approach to account for a trend in geostatistics is based on the decomposition in Formula (1). A preliminary step is modeling the trend m($\mathbf{u}_\alpha$) at all locations $\mathbf{u}_\alpha$. The assumption of second order stationarity is then transferred to the residuals which are calculated at the N sample data locations as $r(\mathbf{u}_\beta) = z(\mathbf{u}_\beta) - m(\mathbf{u}_\beta)$. Multiple geostatistical realizations of the residuals are generated and added back to the trend model. The resulting models of heterogeneity honor the trend.

There are two major deficiencies to this simple decomposition method (see Figure 17). The first is the inability to reproduce heteroscedastic features in the bivariate relationship between the residuals and the trend. Although the simple decomposition accounts for a non-stationary mean, it does not account for a non-stationary variance. The second deficiency is related to the constraint that the residual must be greater than or equal to –m. A simple addition does not ensure Z will be nonnegative at unsampled locations. Both deficiencies must be handled explicitly to ensure plausible results; a stepwise conditional transform of the original variable conditioned by the mean component was proposed for such situations.

5.3. Stepwise Transformation

A stepwise transformation of the trend can be used to account for both heteroscedastic and constraint behavior (Leuangthong and Deutsch, 2004). One way to fix the problems in the classical decomposition is to transform to normal scores the variable of interest conditional to some mean windows:

$$Y_R(\mathbf{u}_\beta) = G^{-1}\left[F\left\{R(\mathbf{u}_\beta) \mid m(\mathbf{u}_\beta)\right\}\right]$$

This amounts to subsetting of the variable of interest (the residual in this case) based on its corresponding trend value. For instance, consider a subset of the trend data ranging from 0.5 to 2.0 trend units (say, % grade or porosity). Examination of the available data shows that there are 53 data pairs of trend data and the corresponding residual that fall within this range. Now apply the normal score transform to the 53 residual data. This same procedure would be carried out for the next range of trend data (say 2.0 to 3.2 trend units), and so forth until all the residual data are transformed. The resulting transformed residuals are independent of the trend component, and hence can be simulated independent of the trend. Back transformation ensures the relationship between the trend and original residual data is reproduced. As in the previous decomposition case, the simulated residuals can be added to the trend to yield simulated realizations of the attribute of interest.

Consider a small reservoir example where we are interested in modeling porosity. Figure 18 shows the location of available wells and the vertical porosity trend that can be found in the wells. We can also see that overall, porosity tends to increase as we move from west to east. Kriging was used to construct a 3D trend model and the areal trend becomes apparent (see Figure 20(left)). Using this trend model, the residual porosity data were then obtained by dissociating the trend from the original porosity data. Figure 21(left) reveals the resulting heteroscedastic and non-linear relationship between the trend and the residual. Stepwise conditional transformation was performed and the transformed residuals and its relationship to the corresponding trend are shown in Figure 19. Gaussian simulation of the residuals was then carried out; the simulated values back transformed; and the residuals added to the trend model. Figure 20 shows a comparison of the trend model and one realization of porosity. We can see an overall reproduction of the trend – the high porosity region is concentrated in the east, while the low porosity region is concentrated in the west. Figure 21 shows good reproduction of the heteroscedastic relationship between the simulated residual and the trend model by using this approach.

In the case of constraint features, the practitioner should consider transforming the original variable conditioned to its trend component. This is especially relevant when the residual data are negative; transforming the original data ensures that any back transformed value will be non-negative.

5.4. Residual Variogram

A common issue that arises in working with residuals in presence of a trend is variography. Since the simulation we will perform will technically be that of the residuals, it is understood that we should model and use the variogram of the residuals in the simulation. However, there are some problems with proceeding in this manner. First, the common procedure is that the residual is modeled independent of the trend and the conventional normal score transform is applied. The complex, dependent relationships we saw in the previous section are not considered, and so the residuals and the trend remain *dependent*. We can see that this dependency has an impact on the covariance of the residuals (following from the decomposition in Equation 1):

$$C_r(\mathbf{h}) = C_z(\mathbf{h}) - C_m(\mathbf{h}) - 2C_{mr}(\mathbf{h})$$

Secondly, even if one were to ignore this correlation between the trend and the residual, the residual variogram tends to be more discontinuous with higher nugget effect and shorter range. This is due to the imposed trend model; if the trend is too variable, that is, with well defined regions of small trends, then the trend captures too much of the variability of the phenomena. This leaves more of the stochastic features to be captured by the residual, and consequently makes it difficult to discern much structure in the residual variogram especially at short scales. The modeler should be careful to avoid capturing too much structure in the trend model; the focus should be to account *only* for large scale trends. Small, regional trends should be left for the residual variable; if there are sufficient data to support such trends, then data conditioning and spatial continuity will dominate and these finer trends will be accounted.

These two issues make variogram modeling in presence of a trend somewhat of an art. One suggestion is to use the variogram of the original variable, especially in instances where inference of the residual variogram is a challenge, particularly at short scale distances. If the trend truly captures only large scale features, then the variogram model associated to the trend is quite smooth and has limited impact at short scales. Using the original variable variogram allows inference of a short scale structure that would otherwise be considered too unstructured for the residual. At larger scales, the original variable variogram can be modeled as stationary.

6. Conclusion

There are several alternatives to consider for building a trend model and honoring the trend within a geostatistical workflow. This work has described and in some cases implemented the most popular ones. There will always be a degree of subjectivity involved in modeling and integrating trends – different geological scenarios call for different trend modeling methods and implementation. However, this work provides options and guidelines for the practitioner.

References

Deutsch, C. *Geostatistical Reservoir Modeling*. Oxford University Press, 2002.

Journel, A. G. *Combining Knowledge from Diverse Sources: An Alternative to Traditional Data Independence Hypotheses.* Mathematical Geology, Vol. 34, No. 5, July 2002.

Journel, A. G. and Huijbregts, Ch. J. *Mining Geostatistics*. The Blackburn Press, Caldwell, N.J., 1978.

Leuangthong, O. and Deutsch, C. V., *Transformation of Residuals to Avoid Artifacts in Geostatistical Modelling with a Trend*, Mathematical Geology, 36 (3), April 2004, pp. 287-305.

Appendix A

Consider the assessment of any unknown event A through its conditional or posterior probability P(A | B, C) given two events B and C where A, B, and C can be any event as long as the prior P(A) and pre-posterior P(A | B) and P(A | C) probabilities can be calculated. The two common approaches for combining the prior and pre-posterior probabilities are to assume that B and C are fully independent or to assume that B and C are incrementally conditionally independent. These are now developed. The A, B, C event notation is used for simplicity; however the derivation is the same for the facies probability p_S framework. The following exact decomposition is the basis for the derivations:

$$P(A \mid B, C) = \frac{P(A, B, C)}{P(B, C)} = \frac{P(A) \cdot P(B \mid A) \cdot P(C \mid A, B)}{P(B, C)} \tag{0.1}$$

The difficulty in the exact solution in (1) is the dependence of events B and C making the evaluation of P(C | A, B) and P(B, C) difficult. The first approach around this limitation is to assume B and C are fully independent, that is:

$$P(C \mid A, B) = P(C \mid A)$$
$$P(B, C) = P(B) \cdot P(C)$$

Equation (0.1) is then simplified:

$$P(A \mid B, C) = \frac{P(A) \cdot P(B \mid A) \cdot P(C \mid A)}{P(B) \cdot P(C)}$$

Using Baye's inversion:

$$P(A \mid B, C) = \frac{P(A \mid B) \cdot P(A \mid C)}{P(A)} \tag{0.2}$$

Equation (0.2) represents the full independence probability combination scheme. The 3D sand facies trend model is calculated by simply scaling or multiplying the horizontal sand proportions by the vertical sand proportions and then standardizing or dividing by the global proportion. This simple relationship is popular among practitioners since it is straightforward to implement; however, it does not ensure the posterior probability $P(A \mid B, C) \in [0, 1]$. In practice, full independence exaggerates low and high probabilities. And of particular concern is the common occurrence of probabilities greater than 1.

The second approach around the B, C dependence limitations in (0.1) is to assume B and C are conditionally independent. The Appendix contains an example intended to illustrate conditional independence within a trend modeling framework. If, conditional to the event A, B and C are independent:

$$P(B, C \mid A) = P(B \mid A) \cdot P(C \mid A)$$

Equation (0.1) is then simplified:

$$P(A \mid B, C) = \frac{P(A) \cdot P(B \mid A) \cdot P(C \mid A)}{P(B, C)} \tag{0.3}$$

The conditional independence simplification does not remove P(B, C), which is difficult to evaluate. Also, equation (0.3) does not ensure the following posterior probability closure:

$$P(A \mid B, C) + P(\bar{A} \mid B, C) = 1.0 \tag{0.4}$$

From equation (0.3), equation (0.4) can be expanded:

$$P(A) \cdot P(B \mid A) \cdot P(C \mid A) + P(\bar{A}) \cdot P(B \mid \bar{A}) \cdot P(C \mid \bar{A}) = P(B, C) \tag{0.5}$$

For (0.4) and (0.5) to be true, the posterior probability P(A | B, C) is standardized:

$$P(A \mid B, C) = \frac{P(A) \cdot P(B \mid A) \cdot P(C \mid A)}{P(A) \cdot P(B \mid A) \cdot P(C \mid A) + P(\bar{A}) \cdot P(B \mid \bar{A}) \cdot P(C \mid \bar{A})} \tag{0.6}$$

$$= \frac{\frac{P(A \mid B) \cdot P(A \mid C)}{P(A)}}{\frac{P(A \mid B) \cdot P(A \mid C)}{P(A)} + \frac{P(\bar{A} \mid B) \cdot P(\bar{A} \mid C)}{P(\bar{A})}}$$

The posterior probability P(A | B, C) can be reshaped:

$$P(A \mid B, C) = \frac{1}{1 + x} = \frac{a}{a + bc} = \frac{x - b}{b} = \frac{c - a}{a} \tag{0.7}$$

with

$$a = \frac{1 - P(A)}{P(A)} \qquad b = \frac{1 - P(A \mid B)}{P(A \mid B)} \qquad c = \frac{1 - P(A \mid C)}{P(A \mid C)} \qquad x = \frac{1 - P(A \mid B, C)}{P(A \mid B, C)}$$

Equation (0.7) represents the permanence of ratios combination scheme. Specifically, $\frac{x - b}{b} = \frac{c - a}{a}$ from (0.7) is referred to as a permanence of ratios. It is interpreted as the incremental contribution of C to A is the same regardless of B or B and C are incrementally conditionally independent. This assumption is less severe than the full independence model and results in legitimate probabilities.

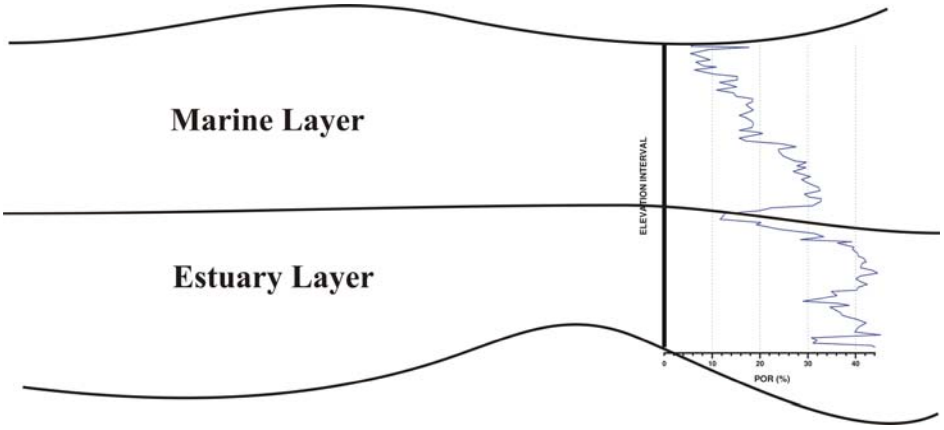

Figure 1 Higher porosity is expected with depth since a brine rich estuary environment existed before the marine environment.

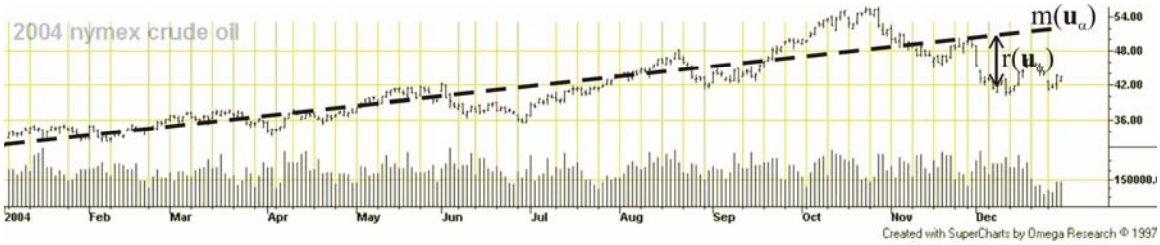

Figure 2 Crude oil prices ($US/barrel) show a clear trend (straight broken line) toward higher prices late in the 2004 year. (Data source: *NYMEX*; Graph Source: *TFC Commodity Charts*)

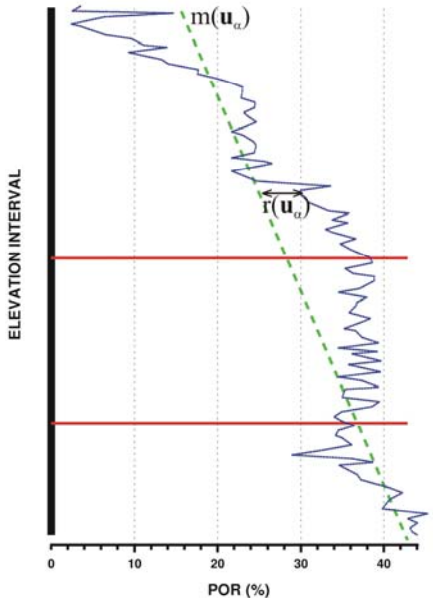

Figure 3 Porosity from a well log show a clear fining upwards trend.

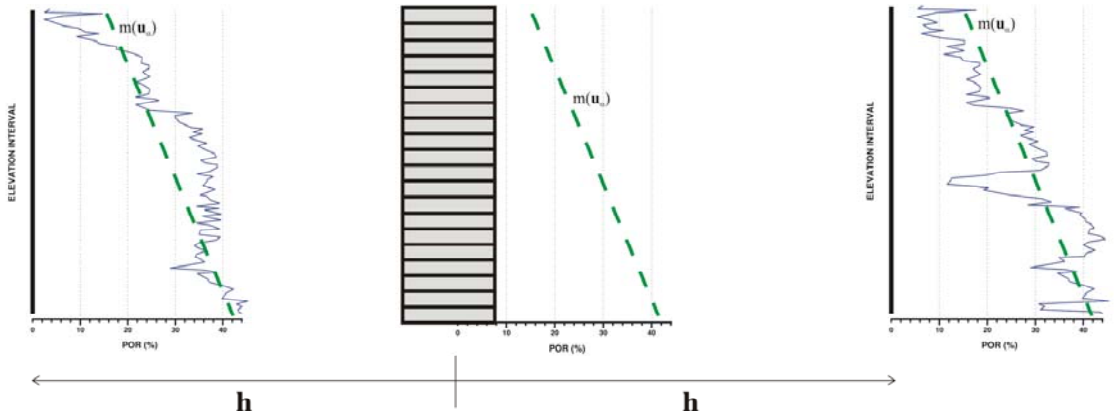

Figure 4 The trend for a vertical string of reservoir blocks can be inferred from the neighboring porosity profiles and an understanding of a geological setting similar to Figure 1.

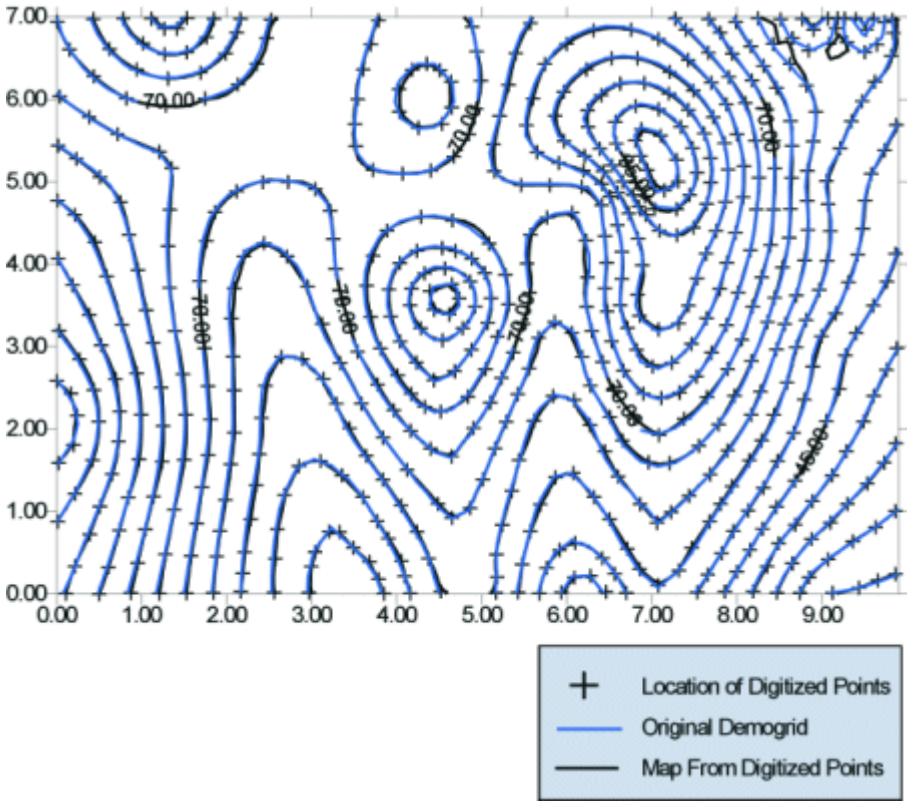

Figure 5 A hand contouring example from Surfer software showing the digitization of hand drawn contour lines. The hand contours are shown as the blue lines and the digitized points and the resulting contour lines from the points are shown as crosses and the black line, respectively.

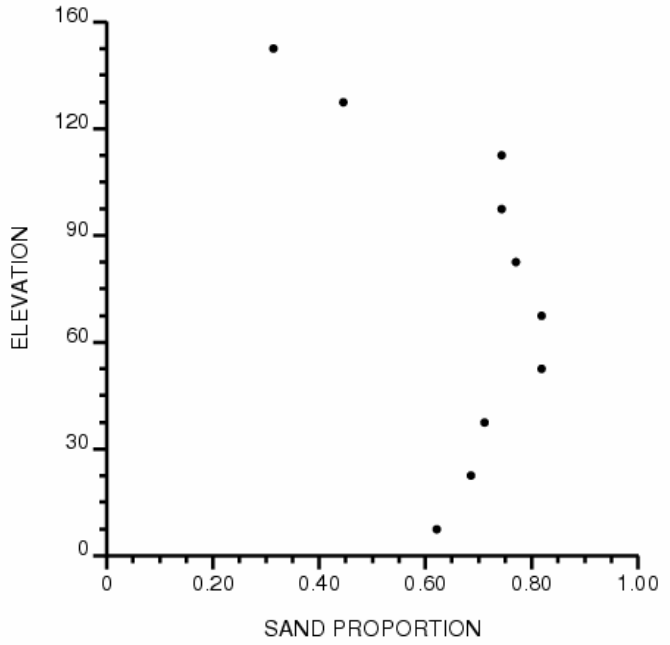

Figure 6 A 1D sand trend calculated from multiple vertical windows. The proportion of sand facies is calculated within each window and plotted against the center of each window.

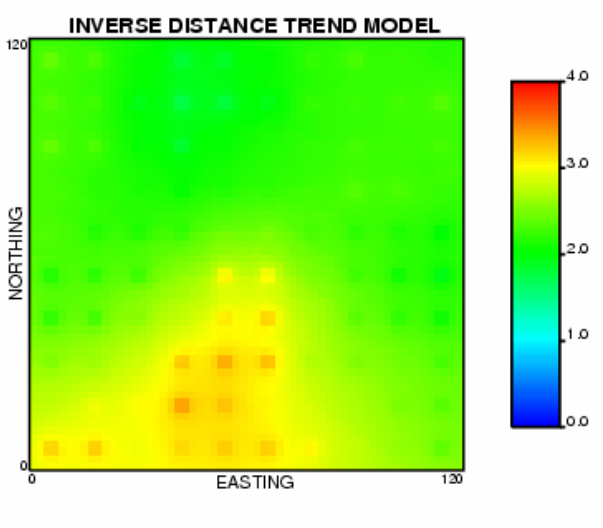

Figure 7 A 2D aerial gold grade trend map created using inverse distance.

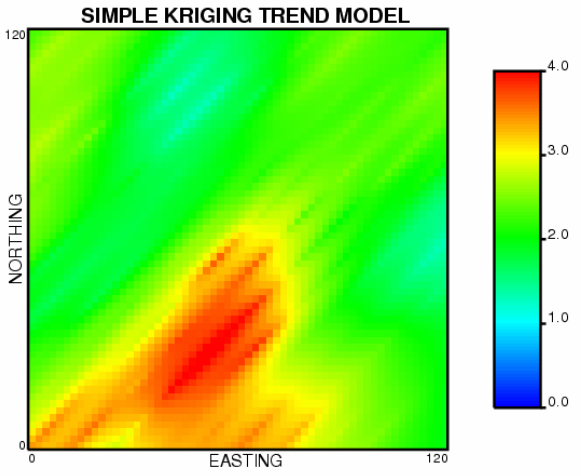

Figure 8 A 2D aerial gold grade trend map created using simple kriging.

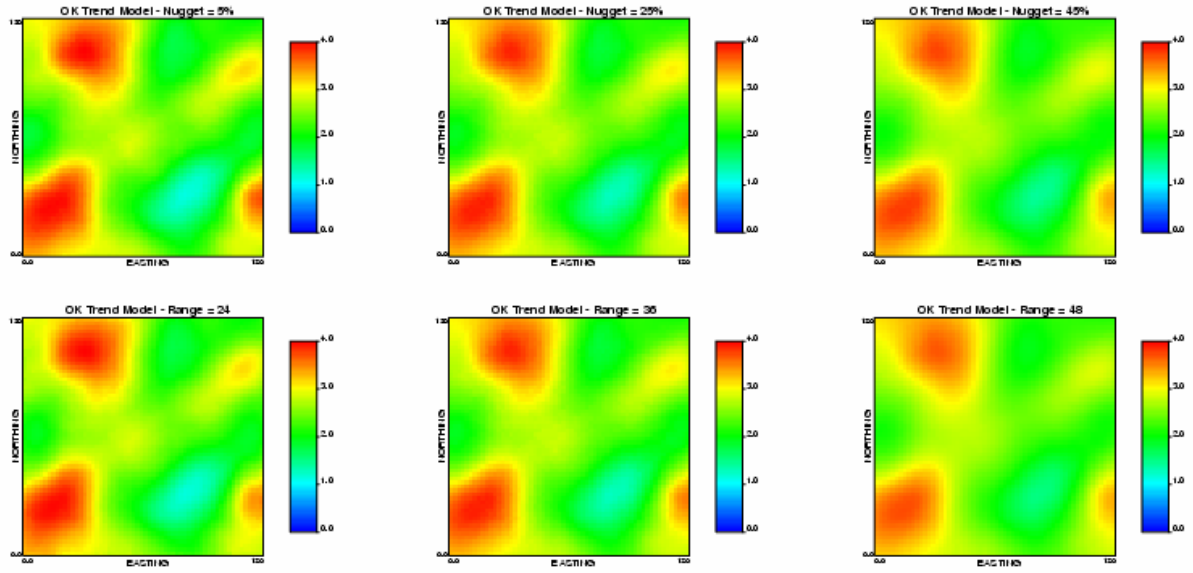

Figure 9 A 2D central plan view slice through a gold grade trend map created using block ordinary kriging.

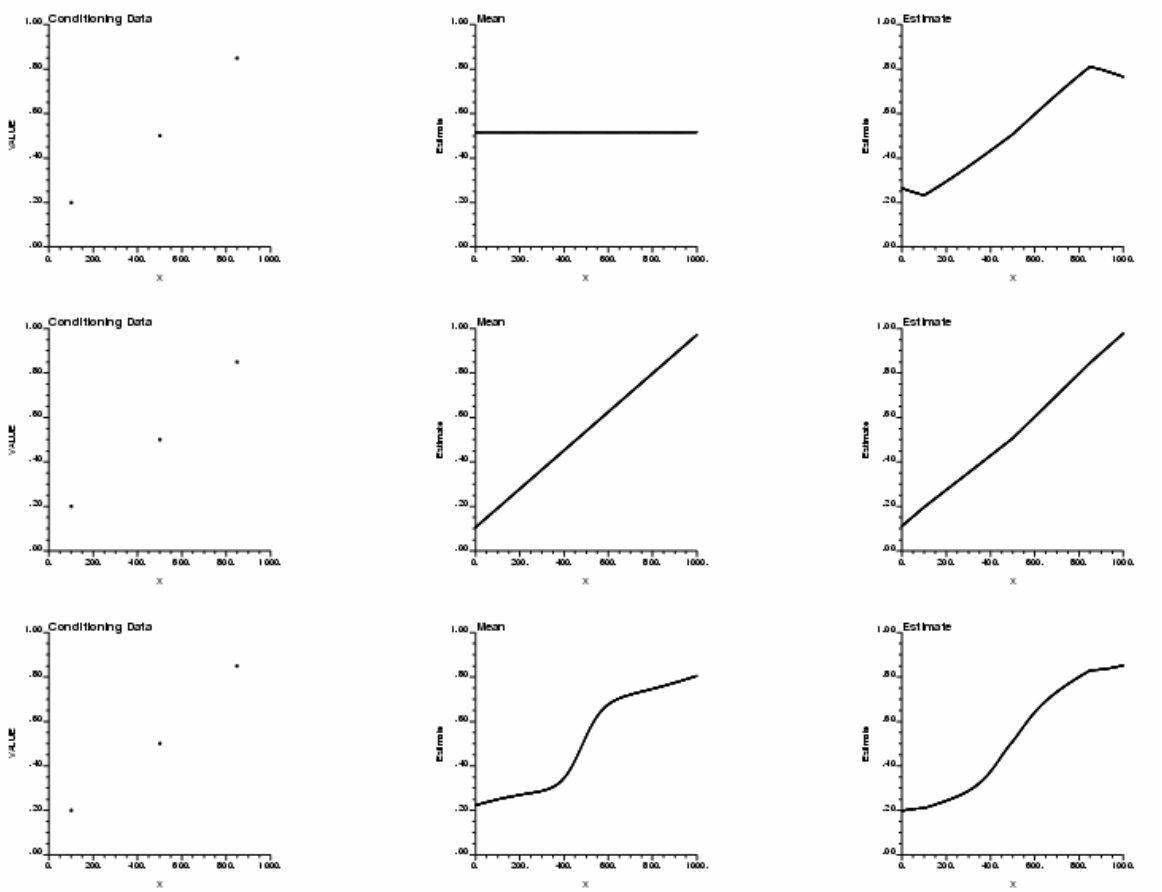

Figure 10 An illustration of trend and attribute estimation using universal kriging in a simple 3 data example.

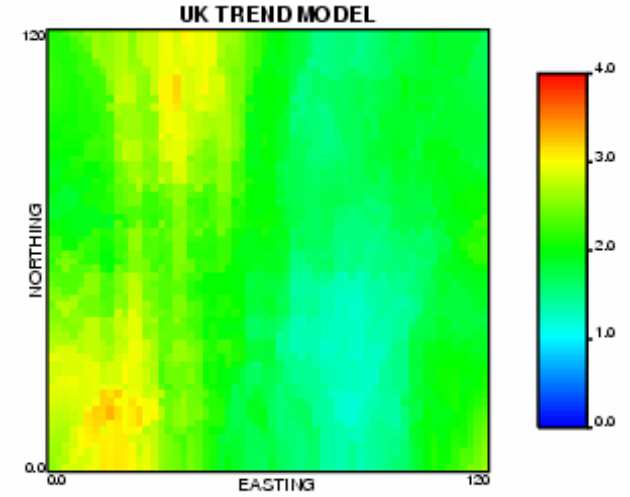

Figure 11 2D central plan view slice through a gold grade trend map created using universal kriging.

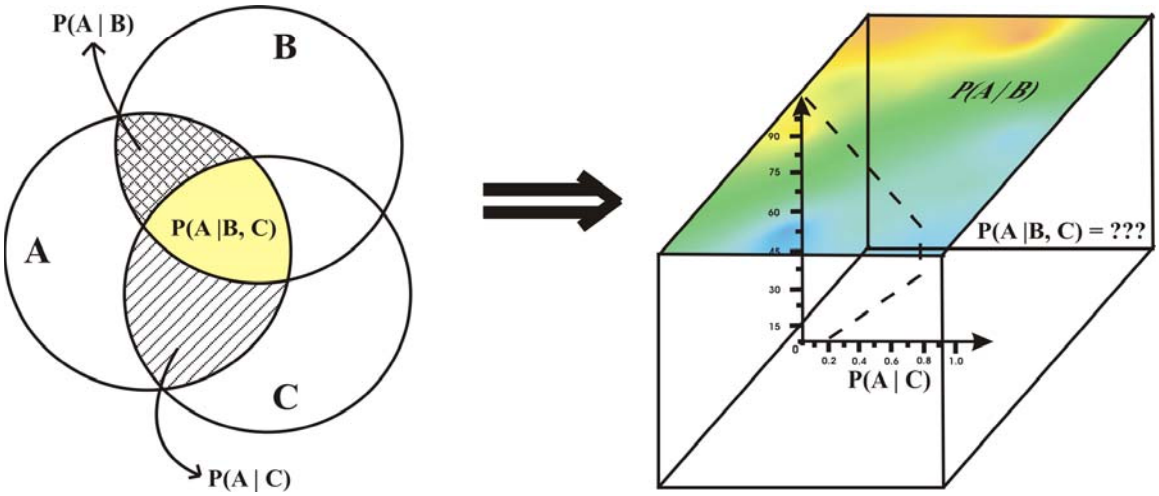

Figure 12 Pre-posterior and posterior probabilities represented as a Venn diagram for events A, B, and C (left) and represented as a facies trend model for events pS(x,y,z) (3D trend model), pS(x,y) (horizontal trend map), and pS(z) (vertical trend curve).

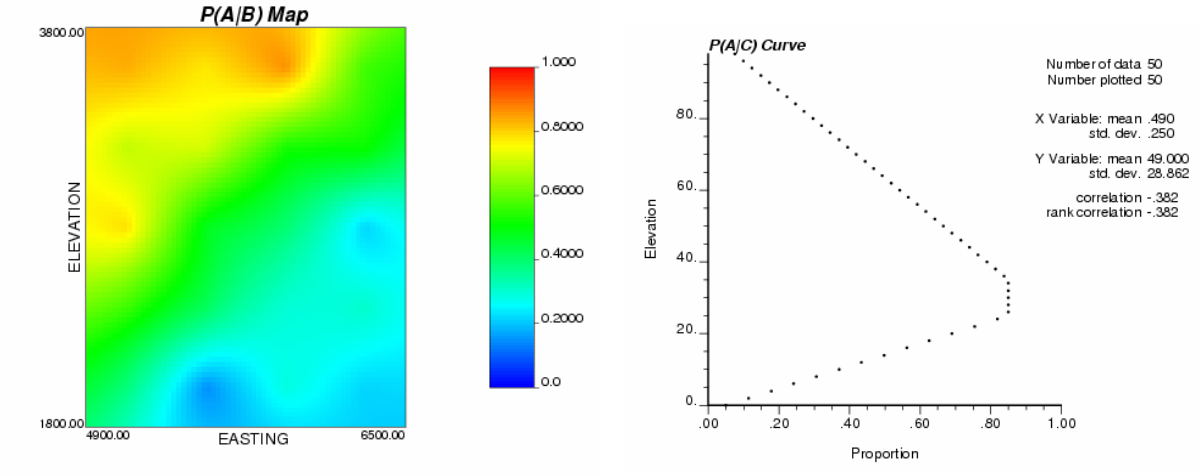

Figure 13 The pre-posterior probability of sand in the aerial plane P(A | B) is shown on the left and the pre-posterior probability of sand in the vertical direction P(A | C) is shown on the right.

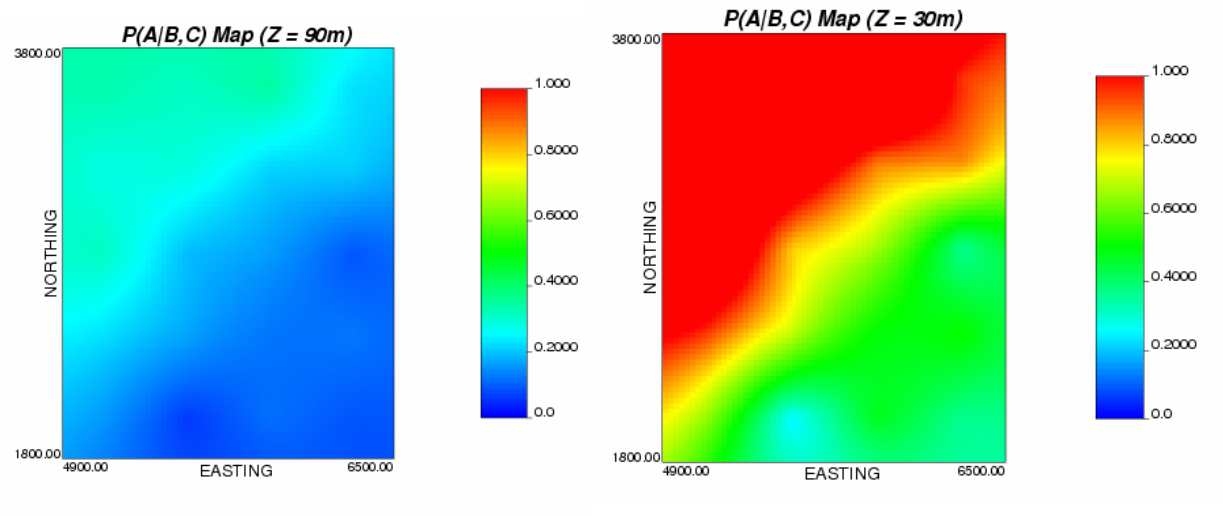

Figure 14 A low value (left) and high value (right) plan view cross section through the posterior probability P(A | B, C) of sand model assuming full independence.

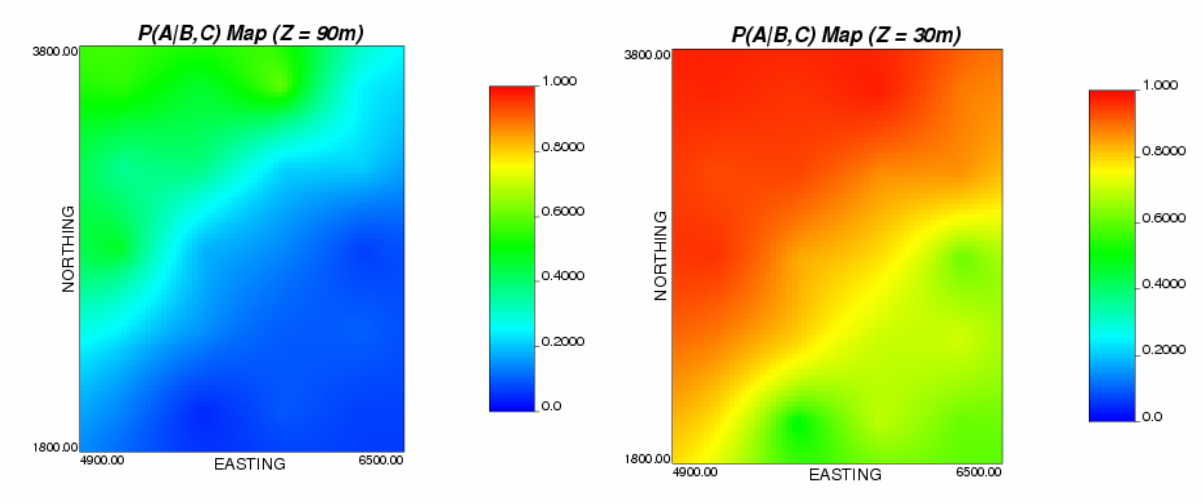

Figure 15 A low value (left) and high value (right) plan view cross section through the posterior probability P(A | B, C) of sand model using permanence of ratios.

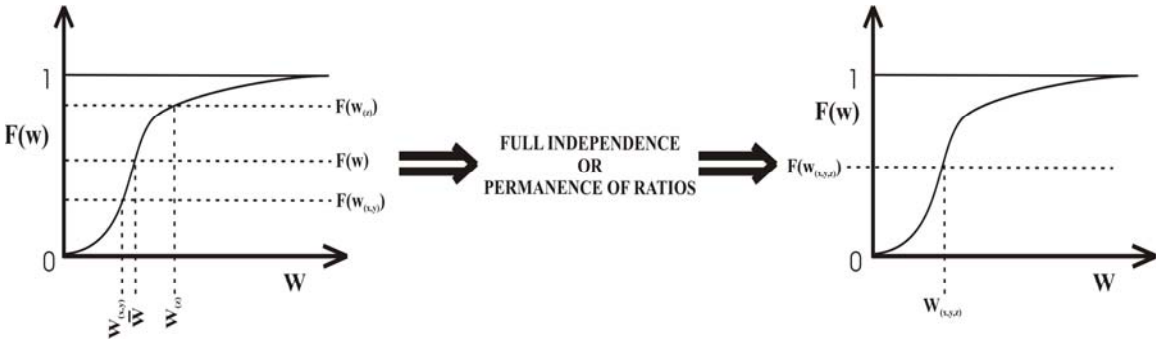

Figure 16 The full independence and permanence of ratios combination scheme for continuous variables.

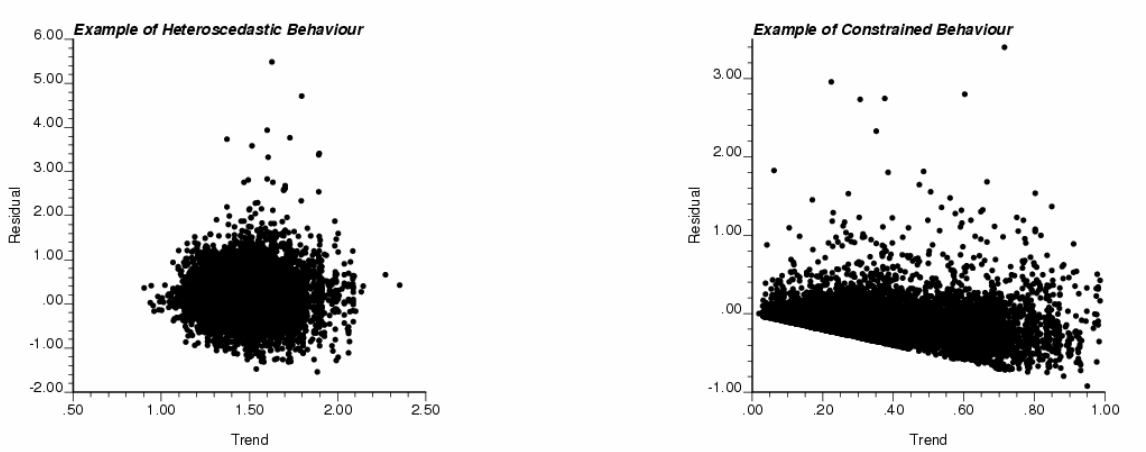

Figure 17 Example of heteroscedastic variance of residuals (left) and constraint (right). (Source: Leuangthong and Deutsch, 2004)

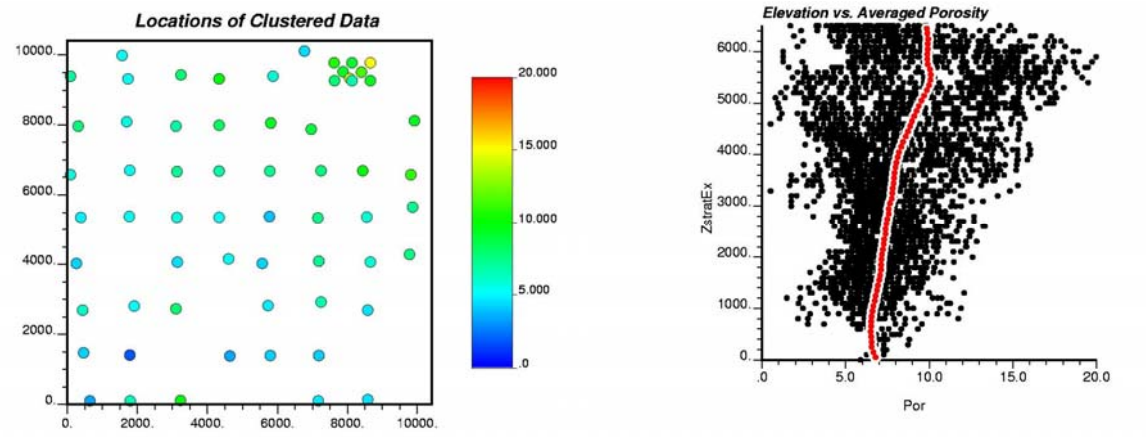

Figure 18 Location map of clustered porosity data (left) and the corresponding vertical trend (right). (Source: Leuangthong and Deutsch, 2004)

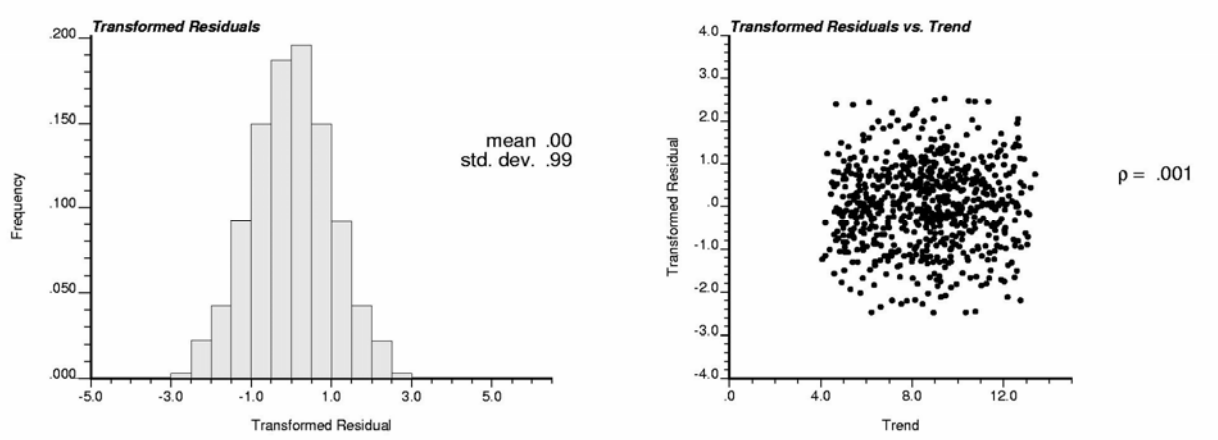

Figure 19 Histogram of stepwise conditionally transformed residuals and corresponding crossplot with the trend. (Source: Leuangthong and Deutsch, 2004)

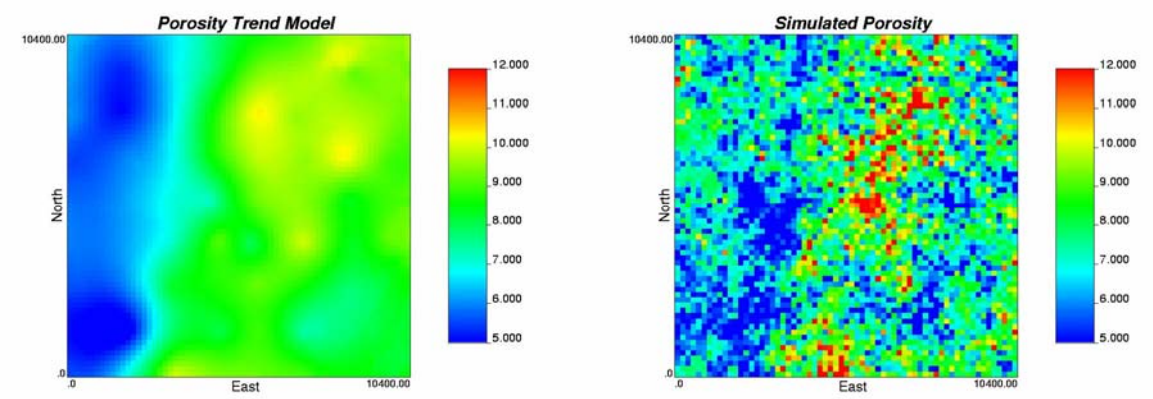

Figure 20 Comparison of porosity trend (left) and one realization of porosity after back transformation of stepwise scores (right). (Source: Leuangthong and Deutsch, 2004)

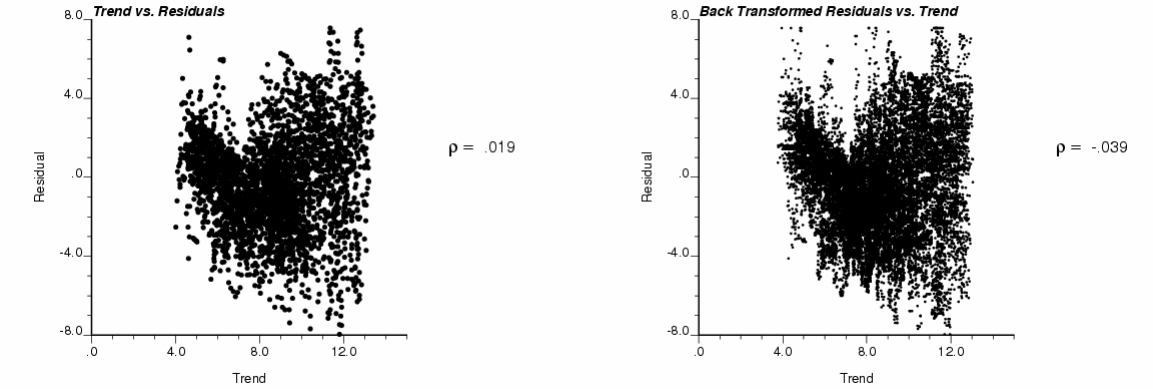

Figure 21 Original porosity trend and residual (left) shows non-linear, heteroscedastic features that are reproduced after applying the transform, simulating and back transforming the stepwise scores (right). (Source: Leuangthong and Deutsch, 2004)